An Efficient Algorithm for Multiple Sclerosis Lesion Segmentation from Brain MRI

5 authors, including:

Rubén Cárdenes
HENSOLDT Sensors
71 PUBLICATIONS   **670** CITATIONS

SEE PROFILE

Simon K Warfield
Harvard University
609 PUBLICATIONS   **21,750** CITATIONS

SEE PROFILE

Elsa M. Macías
Universidad de Las Palmas de Gran Canaria
75 PUBLICATIONS   **315** CITATIONS

SEE PROFILE

Jose Santana
Universidad de Las Palmas de Gran Canaria
9 PUBLICATIONS   **53** CITATIONS

SEE PROFILE

Some of the authors of this publication are also working on these related projects:

Project PhD Thesis View project

Project Real-Time Deformable (non-rigid) Registration for 3D Brain MRI View project

An Efficient Algorithm for Multiple Sclerosis Lesion Segmentation from Brain MRI

Rubén Cárdenes[1,3], Simon K. Warfield[2], Elsa M. Macías[1],
Jose Aurelio Santana[3], Juan Ruiz-Alzola[3,2]

[1] Dept. Ingeniería Telemática, University of Las Palmas de Gran Canaria, SPAIN
[2] Harvard Medical School and Brigham & Women's Hospital, Dept. Radiology, USA
[3] Medical Technology Center, University of Las Palmas de Gran Canaria and Gran
Canaria Dr. Negrín Hospital, SPAIN
E-mail: ruben@ctm.ulpgc.es, warfield@bwh.harvard.edu, elsa@dit.ulpgc.es,
jaurelio@ctm.ulpgc.es, jruiz@ctm.ulpgc.es

Abstract. We propose a novel method for the segmentation of Multiple Sclerosis (MS) lesions in MRI. The method is based on a three-step approach: first a conventional k-NN classifier is applied to pre-classify gray matter (GM), white matter (WM), cerebro-spinal fluid (CSF) and MS lesions from a set of prototypes selected by an expert. Second, the classification of problematic patterns is resolved computing a fast distance transformation (DT) algorithm from the set of prototypes in the Euclidean space defined by the MRI dataset. Finally, a connected component filtering algorithm is used to remove lesion voxels not connected to the real lesions. This method uses distance information together with intensity information to improve the accuracy of lesion segmentation and, thus, it is specially useful when MS lesions have similar intensity values than other tissues. It is also well suited for interactive segmentations due to its efficiency. Results are shown on real MRI data as wall as on a standard database of synthetic images.

1 Introduction

MS lesions have similar MRI intensity levels than other tissues, such as gray matter (GM) in T1 weighted MRI or cerebrospinal fluid (CSF) in T2 weighted MRI, making lesion segmentation and subsequent quantitative analysis a very difficult task. Approaches to tackle this problem include multimodal acquisition of different datasets and atlas registration, in order to take advantage of the fact that lesions only appear inside the white matter [1].

Here we propose a supervised segmentation method based on three steps: (1) k-Nearest Neighbor (k-NN) classification, (2) distance-based intensity overlap resolution, and (3) connected components relabeling.

The k-NN rule [2] is a popular supervised classification method with asymptotic optimum properties, which has been used for years for MRI segmentation due to its good stability conditions [3]. The main disadvantage of this technique is its low execution performance due to the neighbor search, specially in the

multimodal case. The simplest approach, the brute force method, computes for every test pattern, the distances to all the training prototypes and then choses the k nearest ones. This approach is unfeasible for large 3D medical datasets. For this reason several techniques to improve the k-NN performance have been proposed. For example Friedmann [4] ordered the prototypes by increasing distance in every channel and then, the search is reduced to the channel with less local sparsity, reducing the dimensionality of the searching space. Another method is described by Jian-Zhang [5] and Fukunaga [6] which use a branch and bound strategy to find out the nearest neighbors. A very efficient method was proposed by [7], where a fast distance transformation is used to generate a look-up table with the k nearest neighbors directly available. Our k-NN implementation is based on an improved version of this method described in [8].

In order to distinguish different tissues with overlapping intensities, spatial information is added to the method by computing a distance transformation (DT) from the training prototypes. Finally a connected component algorithm is used to remove isolated voxels that are not connected to the real MS lesion.

Indicative execution times are: 0.5 seconds for 256×256 images, and one minute for a full 3D ($181 \times 181 \times 217$) volume.

2 Method

In this work we have chosen a supervised segmentation method, such as the k-NN rule, mainly because it can take into account abnormal anatomy better than unsupervised methods. Some authors have reported unsupervised methods in order to segment abnormal anatomy, as for example tumors detection [9]. Those methods need the introduction of a priori anatomy knowledge in order to detect outliers, and this is achieved usually by means of atlas registration. There are basically two problems with unsupervised methods. The first one is the accuracy, because image registration is an ill posed problem, and thus it is very hard to find voxels belonging to abnormal anatomy among the voxels that are not well registered with an atlas. Usually even for a medical expert it is hard to identify where exactly is located a lesion. The second drawback is the low speed-performance of unsupervised segmentation algorithms, which is also a clear disadvantage.

The k-NN rule is a non-parametric pattern classification technique that has proved to be an excellent method for supervised classification of MRI data. An excellent description of k-NN classification is provided in [10]. Before being applied it requires a training step, carried out by a medical expert by selecting a dataset that consists of a set of classified voxels (training prototypes). Training is carried out in $2-3$ minutes using $100-300$ prototypes, which are usually stored in a file that can be interactively edited in order to improve the segmentation. After training, the method consists of a pipeline with three automatic steps:

2.1 k-NN Pre-Segmentation

The k nearest prototypes of every voxel are searched in order to classify it as class c if most of the k prototypes found belong to class c. A brute force implementation of this algorithm demands a huge computational load and is not feasible for large 3D medical datasets. Thus, we have used a scheme, first described by Warfield [7], where a look-up table is computed by finding out a partition of the feature space into regions such that points in each region have the same k closest prototypes. This partition of the space is denoted as a Voronoi diagram of order k, and if the voxel values are the identifiers of the Voronoi cell centers, this is called the nearest neighbor transform of order k. Some good surveys of the types of Voronoi diagrams and its properties can be found in Okabe et al. [11] and Aurenhammer et al. [12].

In order to compute the k-Voronoi diagrams efficiently we use a novel implementation of a fast algorithm initially proposed by Cuisenaire [8], which is based on a DT by ordered propagation. The concept of ordered propagation to compute DT was introduced by Verwer [13], and the idea is essentially to scan the data from the training prototypes to the rest of the image, i.e., by increasing distance order. For this reason, every voxel in the volume is visited only once to compute the DT as opposed to distance transformations based on mask propagation [14–16], which need several raster scans over the image, and hence voxels are visited more than once. The difference between our approach and that of Cuisenaire is that he uses a technique called *bucket sorting* to store the elements in the propagation scheme, and our implementation uses a *double list* strategy which is less memory consuming and therefore more efficient. The k-Voronoi diagram implementation that we use requires that every pattern is visited k times, obtaining a computational complexity of order $O(k.m)$, i.e. the performance of this approach is linear in the number of patterns in the feature space, m, and linear in k.

Figure 1(a) shows the training prototypes corresponding to a two-channel MRI dataset, (T1w and T2w). The DT from the prototypes, the look-up table for $k = 1$ used in the k-NN classification, and the Voronoi diagram of order one from the prototypes are also shown in 1(b), 1(c) and 1(d) respectively. The lookup table can be interpreted as a partition of the feature space on N_c regions, where N_c is the number of classes, and each region represents a class c, in such a way that a pattern is classified as class c_i if its feature coordinates are located in the region of class c_i at the lookup table. Notice that the lookup table is formed by the junction of the Voronoi cells belonging to the same class. We show the result of the pre-segmentation step with one channel for a T1w MRI coronal slice of the brainweb dataset [17] in figure 3(b), where many voxels belonging to gray matter are misclassified as MS and vice versa due to the overlapping in the intensity space.

2.2 Distance-based Relabeling

The initial k-NN classification using only intensity information is not enough to get good results if there exist tissues with intensity values in the same inten-
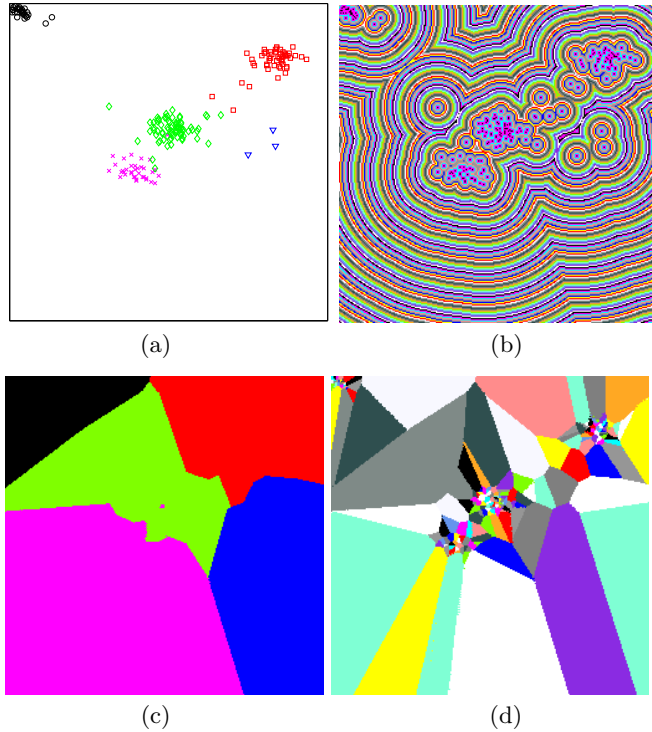
Fig. 1. Training prototype patterns corresponding to a two channel MRI data (a), distance transformation coded with a cyclic colormap from the prototypes (b), lookup table for $k = 1$ (c) and order one Voronoi diagram corresponding to the training prototypes (d)

sity range, as for example gray matter and lesion in T1 weighted MRI. For this reason we propose to separate these ambiguous tissues using additional information. This information is taken here from the spatial location of the training prototypes, in particular, the Euclidean distance from a given pattern to the nearest prototype in the image space. With the addition of spatial information, the patterns to classify becomes of the form $(I_1, .., I_D, dx, dy, dz)$, increasing in 3 the space dimension: $D+3$, where D is the number of channels used. This means that the neighbor search is now in a space of dimension 4 or 5 if the number of channels used are 1 or 2. Searching in a space of dimension higher than 3 is more computationally expensive, more memory consuming and harder to implement. Thus, focusing on efficiency, our method separates intensity and spatial information in different steps. We propose to use a distance-based relabeling step in addition to the previous k-NN pre-segmentation, in order to add the spatial information and distinguish patterns with similar intensity values that belong to different classes.

Let C be the set of classes with overlapping intensity values. If a pattern p is classified as class $c_i \in C$, p will be relabeled, assigning to it the class of the prototype closest to it. This is like adding a new channel of distances d to the k-NN classification in order to resolve the overlap of the classes in the intensity space, as shown schematically in figure 2.

In order to make the relabeling of the pre-classified voxels in an efficient way, the Euclidean distance transformation from the prototypes belonging to the set of overlapping classes C are computed in the whole image. For example, in a T1 weighted MRI, there are two conflicting classes in C: gray matter (c_1) and lesion (c_2). In this case two DTs are computed from the prototypes of both classes. Then a pattern p initially belonging to c_1, will be classified as c_2 if the DT from c_2 prototypes has a lower value at p than the DT from c_1 prototypes. Notice that we prevent mis-classifications of voxels clearly classified, regardless how close in the image are the prototypes of the other classes, by avoiding relabeling voxels outside C, i.e. voxels with no intensity overlapping.

As in the first step, the DT implementation used here is based on ordered propagation with a *double list* strategy in order to be highly efficient. In consequence, the computational complexity in this step is linear in the number of voxels: $O(M)$. Notice that now we need to compute a DT in a 3D space, while in the previous k-NN pre-classification step the lookup table was computed in a domain of dimension equal to the number of channels used, which is usually no more than two. Therefore, the computational load is now higher because M is in general greater than $k.m$. The result of the distance-based relabeling step for the T1w MRI coronal slice of the brainweb dataset is shown in figure 3(c), and the DT used is shown in figure 4 for the GM prototypes and the MS prototypes.
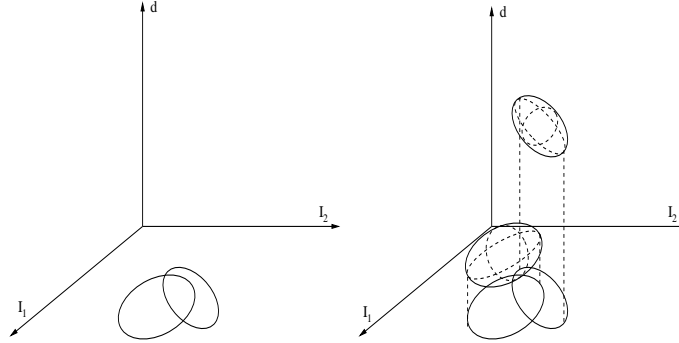

Fig. 2. Two classes overlapped in the feature space I_1 and I_2 (left), and class separation adding the spatial channel d (right)
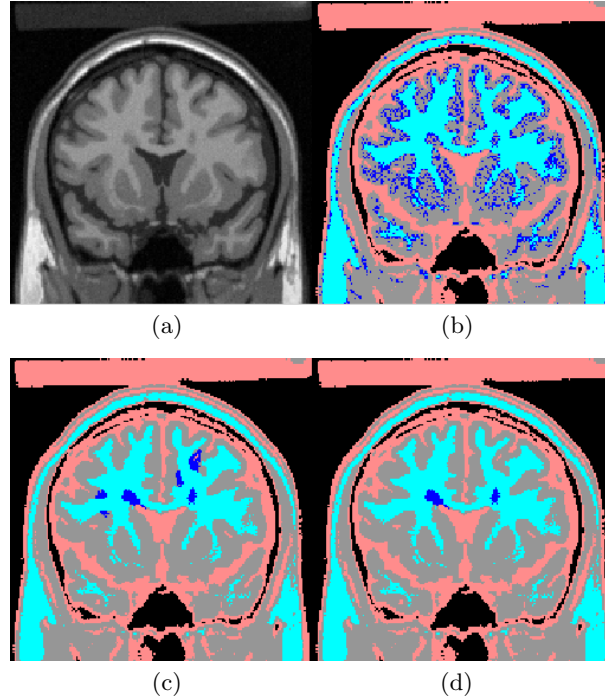
Fig. 3. Source image: T1w MR coronal slice (a). First step: k-NN segmentation with one intensity channel (b). Second step: distance-based relabeling (c). Third step: connected component filtering from MS lesions (d). Color code: Background = black, White Matter = light blue, Gray Matter = gray, CSF = orange, MS = dark blue

2.3 Connected Component Filtering

Still some mis-classifications remain since there are voxels located near lesion prototypes but they do not really belong to lesion, as shown in figure 3(c). This problem appears because the proportion of lesion prototypes respect to the number of voxels that really belong to lesion is high compared to this proportion in other tissues due to the major importance and locality of MS lesions. For this reason many non lesion voxels are mis-classified. The third step corrects this problem, removing the lesion regions not connected to lesion prototypes. This is achieved applying a connected component filter to the classified image starting from the lesion prototypes (see figure 3(d)). It is required to have at least one prototype for every MS lesion connected component, in order to obtain a correct classification with our method.

2.4 Results

In addition to the 2D experiment shown before, we have made 3D experiments using the standard simulated $181 \times 181 \times 217$ MRI brainweb dataset [17] to asses
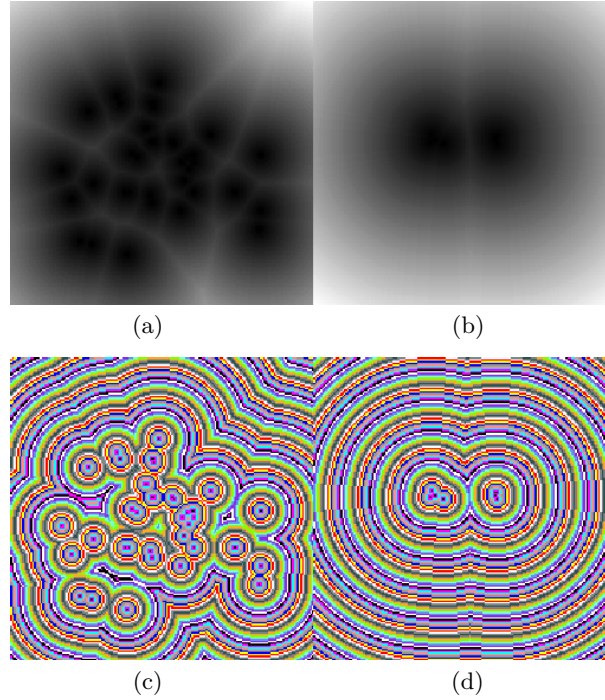
Fig. 4. DT from GM prototypes (a),(c) and from MS prototypes (b),(d) coded in gray scale colormap (top), and coded in a cyclic colormap (bottom)

quantitatively the speed-performance, we illustrate in figure 6 the orthogonal slices of a 3D segmentation with our method. The total CPU times measured in a SUN Ultra-10 workstation with a SPARC II 440 MHz processor and 512 MB RAM, are shown in table 1, as well as the partial times for the different steps in the 2D and 3D experiments. Notice that the second step is the most time consuming one, and the total execution time in the 3D experiment takes less than one minute (59.66 seconds).

Figure 5 shows an example from real MRI data, from a patient with Multiple Sclerosis. The original axial slices PD and T2, show four non connected MS lesions, which are always correctly identified by our method using $k = 5$ and 100 prototypes. Notice that if no distance information is used, multiple MS misclassifications appear in the image, as shown in figure 5 on the left side of the last three rows, moreover when the intensity values are similar to other structures and only one channel is used as in the T2 case shown in the second row of figure 5.
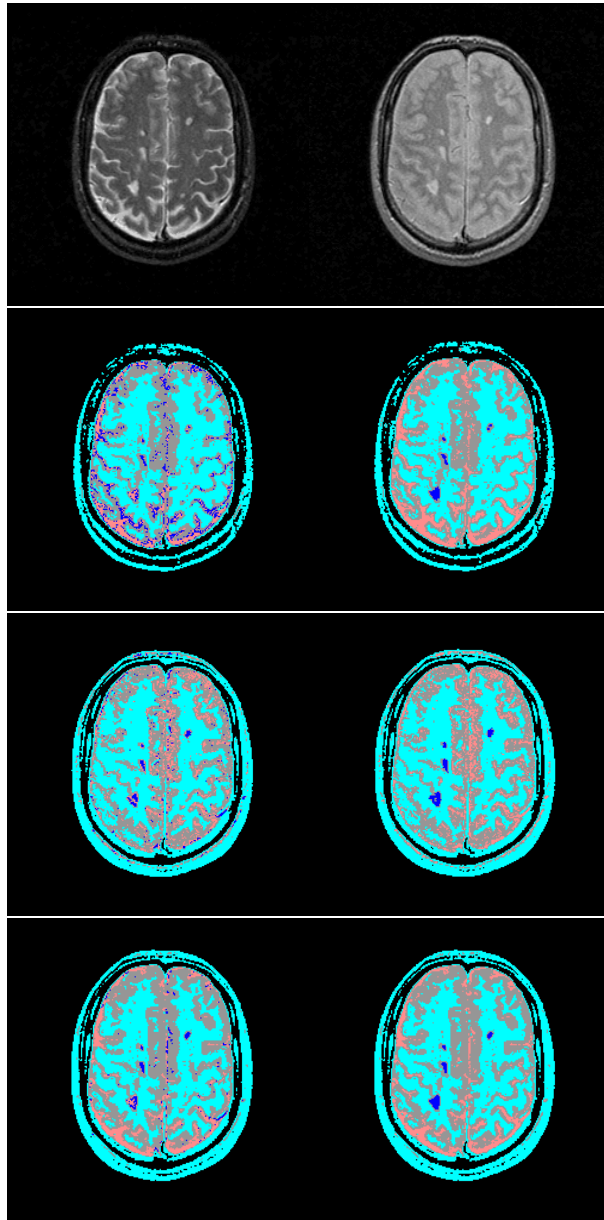
Fig. 5. Top row: axial T2 weighted MRI slice of a patient with MS, (left) and PD weighted (right). Second row: k-NN segmentation using T2 (left) and using T2 plus spatial information (right). Third row: k-NN segmentation using PD (left) and using PD plus spatial information (right). Bottom row: k-NN segmentation using T2 and PD (left) and using PD, T2 plus spatial information (right). Color code: Background = black, White Matter = light blue, Gray Matter = gray, CSF= orange, MS = dark blue
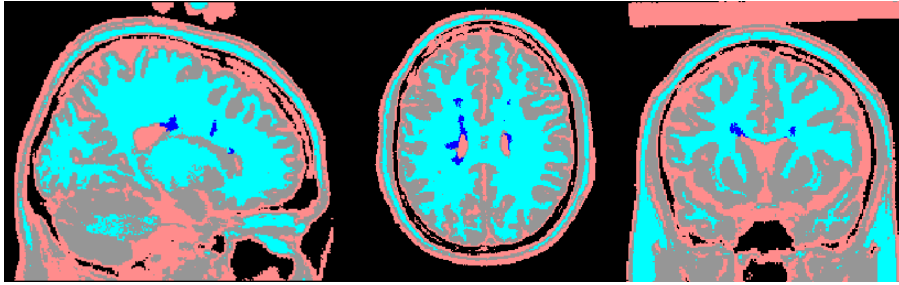
Fig. 6. Orthogonal slices of a 3D segmentation

Table 1. Total and partial execution times in seconds, for the 2D and 3D experiments. Number of prototypes used: 127 in the 2D case, and 390 in the 3D case

	step 1	step 2	step 3	Total
3D (181x181x217)	6.67	52.36	0.63	59.66
2D (181x181)	0.09	0.26	0.002	0.35

3 Conclusions

We have shown a novel high performance method for the segmentation of abnormal anatomy in MRI data, such as MS lesions. One of the main features of this scheme is that it can segment different structures with the same intensity level range. The other principal feature is the high performance achieved due to the fast algorithms to compute distance transformations and Voronoi diagrams on which our method is based on.

Our scheme also shows some advantages with respect to unsupervised methods, because it is fairly stable for the segmentation of abnormal anatomy, and because no image-atlas registration is needed, which is usually a performance bottleneck in other methods. On the other hand, the whole execution time is to be increased around one more minute in order take into account the user interaction to train the classifier.

The algorithm shows a high accuracy, depending essentially on the training dataset selected by a medical expert, and it performs really well using one intensity channel compared to segmentations carried out with more than one channel, which is a clear advantage for clinical applications. It is useful for interactive segmentation due to its high performance and the facility to add or remove training prototypes to improve the results.

The applications of this method go well beyond MS MRI segmentation since it can be used to segment almost every type of image modalities. Currently we are starting to use it for MRI segmentation of the knee cartilage.

Acknowledgments

References

1. Warfield, S., Kaus, M., Jolesz, F., Kikinis, R.: Adaptive, template moderated, spatially varying statistical classification. Medical Image Analisys **4** (2000) 43–55
2. Cover, T., Hart, P.: Nearest neighbor pattern classification. IEEE Transactions on Information Theory **IT-13(1)** (1967) 21–27
3. Clarke, L., Velthuizen, R., Phuphanich, S., Schellenberg, J., Arrington, J., Silbiger, M.: MRI: Stability of three supervised segmentation techniques. Magnetic Resonance Imaging **11** (1993) 95–106
4. Friedman, J., Baskett, F., Shustek, L.: An algorithm for finding nearest neighbors. IEEE Trans. on Computers **C-24(10)** (1975) 1000–1006
5. Jian, Q., Zhang, W.: An improved method for finding nearest neighbors. Pattern Recognition Letters **14** (1993) 531–535
6. Fukunaga, K., Narendra, P.: A branch and bound algorithm for computing k-nearest neighbors. IEEE Transactions On Computers **C-24** (1975) 750–753
7. Warfield, S.: Fast k-nn classification for multichannel image data. Pattern Recognition Letters **17(7)** (1996) 713–721
8. Cuisenaire, O., Macq, B.: Fast k-nn classification with an optimal k-distance transformation algorithm. Proc. 10th European Signal Processing Conf. (2000) 1365–1368
9. Kaus, M.: Contributions to the Automated Segmentation of Brain Tumors in MRI. PhD thesis, Berlin, Germany (2000)
10. Duda, R., Hart, P.: Pattern Classification and Scene Analysis. John Wiley &amp (1973)
11. Okabe, A., Boots, B., Sugihara, K.: Spatial Tesselations: Concepts and Applications of Voronoi Diagrams. Wiley (1992)
12. Aurenhammer, F., Klein, R.: Voronoi diagrams. In Sack, J., Urrutia, G., eds.: Handbook of Computational Geometry. Elsevier Science Publishing (2000) 201–290
13. Verwer, B., Verbeek, P., Dekker, S.: An efficient uniform cost algorithm applied to distance transforms. IEEE Transactions on Pattern Analysis an Machine Intelligence **11(4)** (1989) 425–429
14. Borgefors, G.: Distance transformations in arbitrary dimensions. Computer Vision, Graphics and Image Processing **27** (1984) 321–345
15. Danielsson, P.: Euclidean distance mapping. Comput. Graph. Image Process. **14** (1980) 227–248
16. Ragnemalm, I.: The Euclidean distance transform in arbitrary dimensions. Pattern Recognition Letters **14** (1993) 883–888
17. Cocosco, C., Kollokian, V., Kwan, R.S., Evans, A.: Brainweb: online interface to a 3D MRI simulated brain database. In: Neuroimage. Volume 5 of 425., Copenhagen (1997)